



Numerical investigation of ground tanks for storage subjected near-fault earthquakes

Zakia Tabatabaei¹ and Bahador Fatehi-Nobarian^{2*} 

¹ Civil Engineering of Hydraulic Structures, Department of Islamic Azad University, Tabriz Branch, Tabriz, Iran

² Department of Civil Engineering of Hydraulic Structures, Aras Branch, Islamic Azad University, Jolfa, Iran

Received: January 4, 2021 • Revised manuscript received: July 11, 2021 • Accepted: August 2, 2021

Published online: December 13, 2021

ABSTRACT

Finite element method is known as the most common methods in a numerical analysis of reservoirs subjected to the influence of an earthquake. Investigating the effects of interaction between structures and fluid during the earthquake is among the major objectives of the present research. In this article, by selecting a variety of conventional modes of fluid storage, the dynamic effects of the reservoir and their mutual effects based on changes in physical parameters are analyzed. Unexpectedly, based on the results of this study, it was observed that the crisis situation always does not occur in the full state of the tank. Moreover, the filled and semi-filled reservoirs require seismic retrofitting for mode 10% below the tank height.

KEYWORDS

structure interaction, fluid-storage, ground tanks, dynamic behavior, hydrostatic pressure

1. INTRODUCTION

With regard to the fact that the earthquake phenomenon as a huge lateral force may impose a significant destruction on the structure, particularly on the hydraulic structures, and considering the fact that water storage tanks are highly important structure, therefore it is essential to study the impact of earthquake of near and far faults on the water storage tanks. Priestley et al. [1] have focused on the seismic design of storage in a convenient form as a code of professional standards for the design, load, under the design level earthquake. Later Shri-mali and Jangid [2] studied the separated liquid storage tanks subjected to the two horizontal components of earthquake ground motion and they concluded that the effectiveness of separation systems for tanks increases, due to the increase in system flexibility enhancement. Livaoglu [3] have studied the dynamic behavior of the rectangular liquid reservoir and they claimed that the reservoir exhibits high rate of behavior variation in the soft soil. Seleemah and Sharkawy [4] studied the seismic response of cylindrical liquid storage with a base (support), which was located on plain (smooth) surface and they observed that the detachment of bases have led to the reduction in effects of earthquake on the tank. Liu et al. [5] adopted finite element for investigating the mathematical model devised for analysis of the tank.

Said and Abdulmuttalib [6] used a rectangular tanks for storage and he declared the displacement and axial force components above half-full tanks and empty tanks is equal to (31%) and 75%, respectively. Uddin [7] critically reviewed forces exerted on container systems and it was observed that there is a maximum increase of 15% and 25% in hydrodynamic pressures for elevated tanks and ground supported tanks, respectively. Cacciatore et al. [8] investigated the seismic behavior of liquid storage tank incorporating floating roof under dynamic behavior, geometrical materials, non-linear behavior and El-Zeiny [9] investigated the effects of fluid pressure on the sidewall of unbraced tank during the vibrations induced by earthquakes. Mohammadzadeh et al. [10] studied the calibrated model located in the south

basis of Caspian Sea with main aim of assessing the climate change and its effect on surface water resources. Kia et al. [11] modelled the domain of seismic fluctuations upon the maximum and minimum thickness of the reservoir wall using highly complex mathematical formulas. A sample of steel storage tanks used for water distribution is illustrated in Fig. 1. Neagu et al. [17] have studied the wall systems of steel storage tanks for fluid retention and the benefits of earthquake resistance and lateral forces, including capacity and loss. Zhao [18] has studied and numerically simulated to estimate the appropriate criterion for temperature changes in fluid oils stored in terrestrial. Bába and Karches [19] have studied the presentation of a suitable method for the performance of wastewater treatment and its surface measurement in terrestrial reservoirs in which the batch reactor performance sequence has been studied to optimize the behavior of wastewater flow. In this study, with a main focus on the rectangular tank, serious limitations in the space available to install a water tank were observed. Sleeping cubic tanks are for spaces with height restrictions and book tanks are for spaces that have a small width. Moreover, the cubic tanks have good durability in terms of appearance. These tanks are usually in line so that they can neutralize the impact of fluctuations or fluid consumption. Abacus software has capabilities like explicit and implicit solution procedures, having advanced and diverse behavioral models for different materials, the ability to quickly create models etc. Other features of Abacus include how to solve problems in this software. In complex analyzes, in which it is difficult to predict the process of change, and the process of solving the problem, the ability to automatically adjust time patterns can be used. So, another reason for the growing popularity of this software is the relatively simple and fast way to perform simulation.

2. EQUATIONS DYNAMIC PRESSURE IN TANKS

It is essential to consider the seismic loads for vertical cubic tanks used for storing liquid materials. The dynamic designation pressure induced by strike P_W is determined using seismic coefficient modification method and the dynamic designation pressure P_W is obtained from Eqs (1) and (2), in

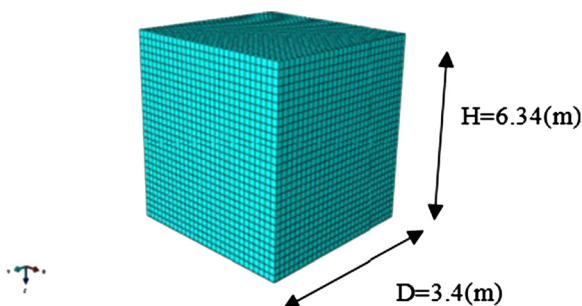


Fig. 1. Water with dimensions, $D = 3.40$ m, $H = 6.34$ m, $H/D = 0.5$ m

which shear forces of dynamic designation resulted from the impact of rocking fluid mass, are sum of seismic force components within the range of internal wall of the reservoir.

The dynamic impact design pressure is

$$P_W = C_e \cdot P_{wop}, \quad (1)$$

where

$$C_e = Z_s \cdot I \cdot D_s S_{a1} / g \quad (2)$$

denotes the shear force coefficient. The dynamic design pressure is

$$P_s = \frac{\eta_s \cdot P_{so}}{D}. \quad (3)$$

The swing wave height is

$$\eta_s = 0.802 \cdot Z_s \cdot I \cdot S_{v1} \sqrt{\frac{D}{g} \tanh\left(\frac{3.682 H_1}{D}\right)}, \quad (4)$$

where Z_s represents the coefficient of the area; I refers to switch factor; and D_s denotes structure. P_{wop} is the reference dynamic pressure, $g = 9.81 \text{ ms}^{-2}$ denotes gravity acceleration; D refers to the side of cubic tank (m). S_{a1} represents the water response spectrum for the first natural period (ms^{-1}), h_s denotes the fluctuations of wave height (m). P_{so} is dynamic pressure of mass (Nmm^{-2}), H refers to the height of stored fluid (m) and S_{v1} represents the design velocity spectrum [12, 13].

2.1. Discussion

In this research, ABAQUS software with the definition of the geometry and the appropriate meshing dimensions is used for analyses and the process is accomplished with $(16 \times 21.1 = 337.6)$ [14]. In a study of Ismail et al. [15], a numerical study that evaluates different possible techniques for the seismic retrofit of existing steel moment-resisting frame structures was conducted. In this paper, three retrofit techniques were proposed, including

- X-Steel braces;
- buckling restrained composite braces; and
- composite concrete-steel plate shear walls [15].

For cylindrical specimens fabrication, limestone powder, sand and high early strength cement were used. The results deduced from finite element analysis demonstrated that the suggested model is efficient in foretelling the compressive behavior of cement-treated sand [16].

In Table 1 the values based on dimension of the Sattar Khan reservoir, which were used for meshing the tank of the present study, are presented.

With regard to the type of the selected models, the selected meshing is a structure with 4-node shell elements and S4R properties (4-node element from plate group), which is suitable for common applications of plate analysis and they have reduced formulation with capability to control the phenomena, limited or membrane strains and dimensions of water for use in the tank are depicted in Fig. 2.

The tank was studied for gaining insight into its behavior under different conditions, ranging from “wall thickness

Table 1. Profile analyses were performed to determine the optimum mesh size steel tanks

The maximum stress in the tank (Pa)	The number of mesh	Mesh size of tank	Geometric dimensions of tank
216326310	680	150 cm	$H/D = 0.5$ ($H = 2D = 6.34/3.40$ m)
247554000	1,888	75 cm	
249064310	17,296	25 cm	

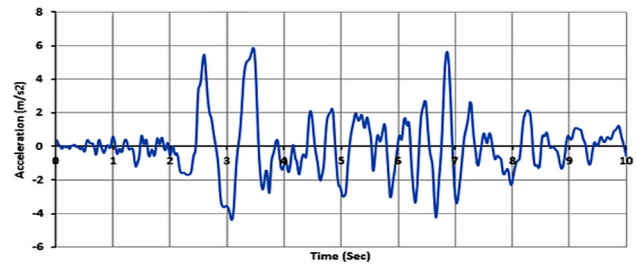


Fig. 2. Earthquake record in X direction

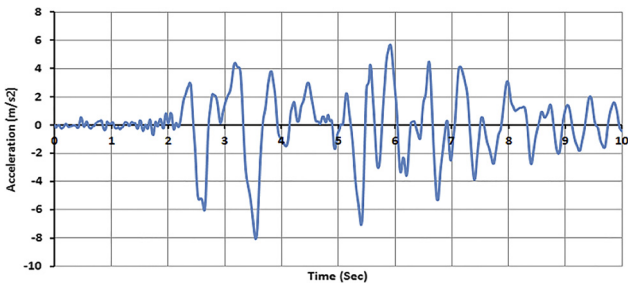


Fig. 3. Earthquake record in the Y direction

changes” and finally, the free surface changes of the fluid inside the tank (fill) and “changes in the velocity of the tank” during 16 analyses and the obtained results are summarized in Table 2, where, H refers to height of the tank, h denotes height of the water and D refers to the side of the tank.

3. METHODOLOGY

In the present research, 16 reservoirs with dimensions of $a = 3.7$ m in side, $h = 6.8$ m in height and various thicknesses, including 0.15, 0.18, 0.20 and 0.22 mm containing waters with two different heights $H/h = 0.5$ and $H/h = 0.6$ with $H/D = 0.5$, were studied in two various accelerations (0.45 and 0.35 ms^{-2}) with two distances near to the fault using Lagrangian-Lagrangian method. Then, the obtained results were compared with data obtained for Sattar Khan

Dam. The data close to that of Sattar Khan Dam, were regarded as the verified data of the research with regard to the information on earthquakes records for various zones, obtained from Institute of Geophysics, Tehran, University, the San Fernando earthquake (far-fault earthquake) and Loma Prieta earthquake (near-fault earthquake) were considered for analyzing the all modes of the reservoir during modeling phase. The bottom the tank is rigid on the basis of the reference point defined for the rigid floor, and the earthquake acceleration in two orthogonal directions. Figures 3 and 4 depict the earthquake record in two axes (X and Y).

To verify the results of the numerical analysis of the model analyzed in this study, the Sattar Khan Earth Dam model will be selected as the basis for the selection studies, and in case of comparison of results, the accuracy of the

Table 2. Definitions and properties of tank

Tank No	Thick-Wall Tank (mm)				Acceleration (m/s^2)		H/h	
	0.15	0.18	0.20	0.22	0.35	0.45	0.50	0.60
1								
2								
3								
4								
5								
6								
7								
8								
9								
10								
11								
12								
13								
14								
15								
16								



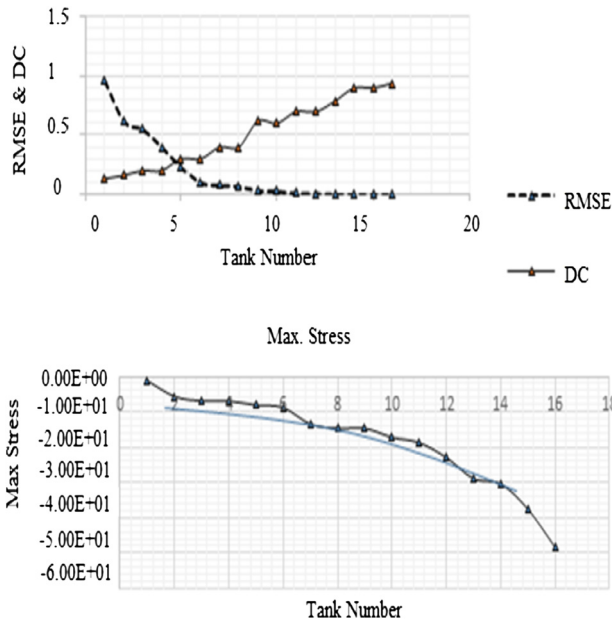


Fig. 4. Diagram RMSE and DC Maximum stresses developed in the reservoir during loading time

studies on other numerical models is determined. Table 3 presents the validation of data with the existing regulations.

4. STRESS RESPONSES OF GROUND TANK WALL

To investigate the dynamic response of the reservoir wall, *RMSE* and *DC* values are obtained for all data using Eqs (5) and (6):

$$RMSE = \sqrt{\frac{1}{N} \left(\sum (S_n - \hat{S}_n)^2 \right)}, \quad (5)$$

$$DC = 1 - \frac{\sum (S_n - \hat{S}_n)^2}{\sum (S_n - \bar{S}_n)^2}, \quad (6)$$

where S_n denotes computed data, \hat{S}_n refers to observational data and \bar{S}_n is average observation data. Figures 4, 5 and 6 illustrate the maximum and minimum tension in the tank during loading and vibration. It should be mentioned that,

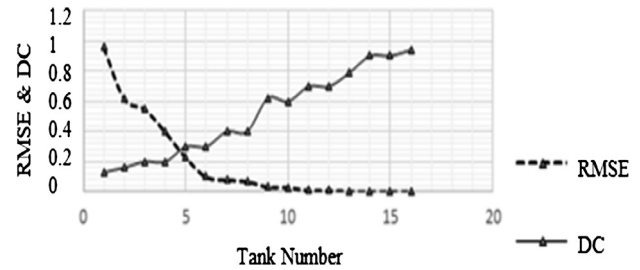


Fig. 5. Diagram RMSE and DC minimum stresses developed in the reservoir during loading time

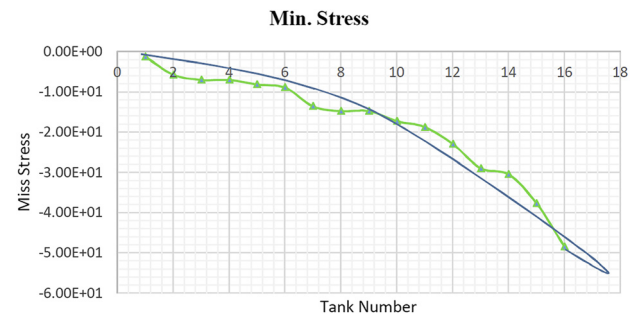


Fig. 6. Minimum stresses developed in the reservoir wall during loading

the diagrams are considered without dimension to make comparisons easier. It was observed that the maximum stress generated in the tank No. 1 is equal to 229 MPa and minimum stress is associated with the tank No. 16 with value of 28.3 MPa. With regard to Table 1, Figs 3 and 4 of *RMSE* and *DC* for maximum stress, it is obvious that the maximum stress with value of 2.3 is attributed to the Tank 1 and the minimum stress with value of 0.003 belongs to Tank 1. Therefore for design considerations, it should be considered that, by increasing the thickness of the wall, the stress-induced tension in the tank structure is not sufficient for control.

With regard to Fig. 5, it is evident that the maximum value, which is equal to 0.96 is attributed to tank 16 and tank 16 possesses the maximum value of -1.17 MPa (minimum stress diagram), while the lowest value which is equal to 0.0001 *RMSE* belongs to tank 16. Again, the lowest stress of minimum stress diagram is attributed to tank 16 with value of -0.4338 .

Table 3. Coefficients and values used as analytical parameters of reservoir structure for calculating and extracting results

Wall thickness	tw	0.02	m	Raging hard mass	$h/D = 0.44$	W_1/W	0.4
Thick roof	tr	0.02	m			W_2/W	0.4
Water lever	h	0.05	m			h_1/D_h	0.5
The side of the tank	O	14.60	m			h_1/h	0.8
Ceiling height	hr	14.60	m			h_2/h	0.6
Acceleration of the plan	A	2.90	($g = 0.30$)	Depending on the number		h_2'/h	0.9
Important factor	I	1.20	-			K_t	0.9 m
Structural behavior factor	R	6.00	-			TO	0.3 sec
Specific gravity of the liquid	η	9,810	Nm^{-3}				
Specific gravity chamber	η	77,009	Nm^{-3}				



5. THE EFFECT OF STRAIN OF GROUND TANK

Considering that strains at the bottom of the tank are of tensile type (with positive number) or as pressure (with negative numbers), Figs 7–10 display the maximum and minimum strain at the bottom of the tank during loading time.

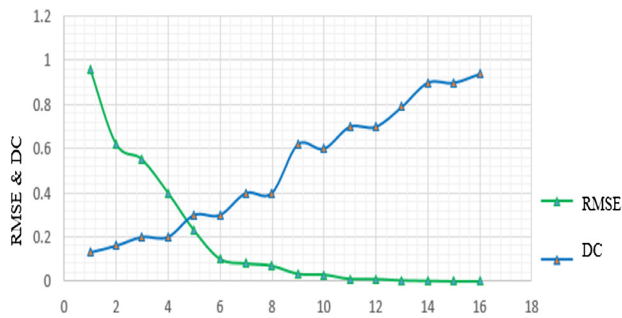


Fig. 7. Diagram RMSE and DC maximum strain developed in the reservoir during loading time

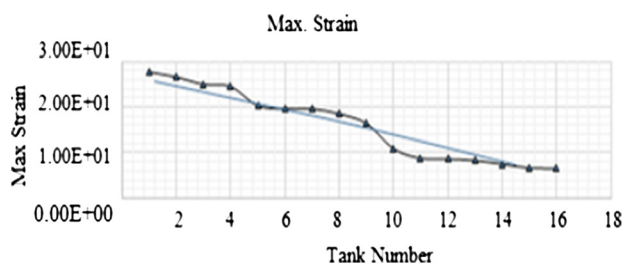


Fig. 8. Maximum strain developed in the reservoir wall during loading

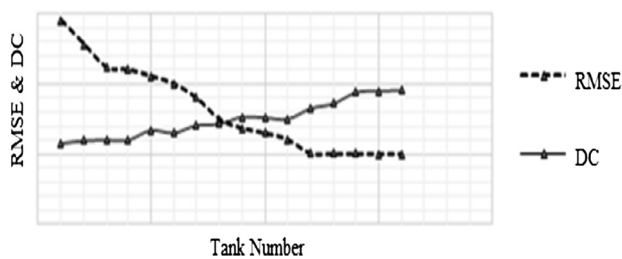


Fig. 9. Diagram RMSE and DC minimum strain developed in the reservoir wall during loading

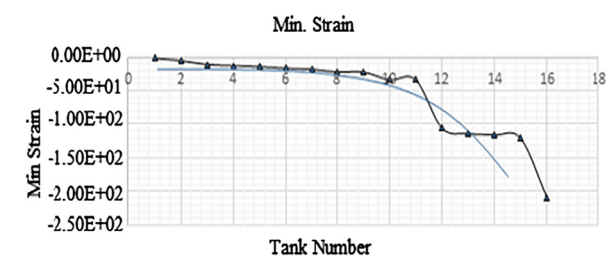


Fig. 10. Strain developed in the reservoir during loading time

6. EFFECT OF CHANGES IN GROUND DISPLACEMENT RESPONSE

Figures 11 and 12 represent the maximum sidewall displacement of the tank in X and Y directions. Moreover, Figs 13 and 14 show the minimum element sidewall movement of the tank with similar conditions for drags (X and Y directions).

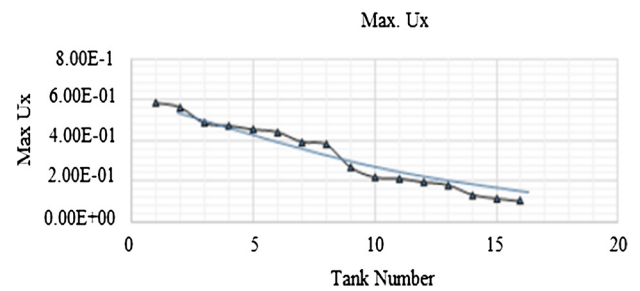


Fig. 11. Push of maximum displacements for elements of tank wall during loading in X direction

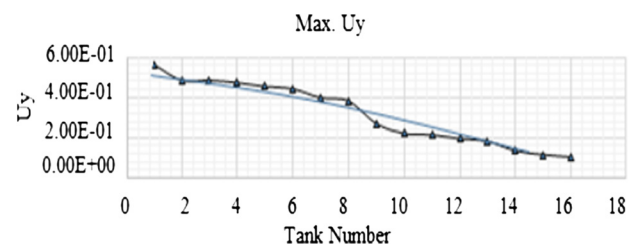


Fig. 12. Push of maximum displacements for elements of tank wall during loading in Y direction

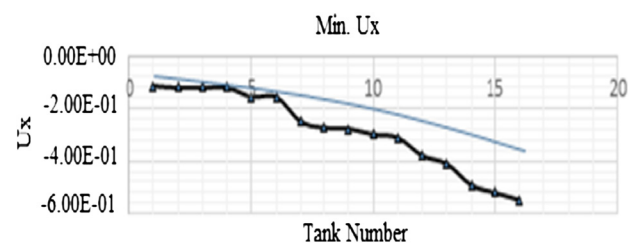


Fig. 13. Push of minimum displacements for elements of tank wall during loading in X direction

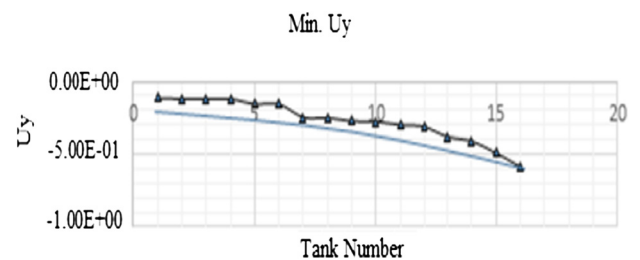
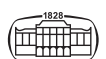


Fig. 14. Push of minimum displacements for elements of tank wall during loading in Y direction



In general, it is observed that during the time of the earthquake, tanks with thicker sidewall undergo more displacement than tanks with less thickness.

7. CONCLUSION

1. Comparison between diagrams of 11 through 14, revealed that the filled tank undergoes more strains. This may be due to increased hydrostatic pressure forces in static conditions, as well as increased reservoir hydrodynamic pressure forces in terms of dynamic reservoir stimulation;
2. Generally, it was observed that the maximum displacements in specific directions are influenced by conditions and amount of acceleration supplied as an input to the models system. So that, the high positive displacements rate belong to semi-filled mode of the tank in both directions (+X and +Y), while, the high negative displacements belong to the completely filled mode of the tank and semi-filled mode of the tank, for directions (−X) and (−Y), respectively;
3. The tanks exhibited significant alterations under the acceleration close to the fault, while they did not experience considerable variation during the acceleration distanced from fault;
4. With regard to the displacements diagram, the surface wave within the reservoir and the animation obtained from analyses, the surface wave continues till the depth of the tank, which is not true for real-world cases except for shallow water conditions in which the depth to diameter ratio of the tank should be less than a specific limit;
5. It was observed that semi-full tanks exhibit more distortion than full and empty tanks;
6. Full and semi-full tanks at levels up to approximately 10% of the tank height, deserves a special attention for seismic resistance.

REFERENCES

- [1] M. J. N. Priestley, J. H. Wood, and B. J. Davidson, "Seismic design of storage tanks," *Bull. New Zealand Natl. Soc. Earthquake Eng.*, vol. 19, no. 4, pp. 272–284, 1986.
- [2] M. K. Shrimali and R. S. Jangid, "Seismic response of liquid storage tanks isolated by sliding bearings," *Eng. Structures*, vol. 24, no. 7, pp. 909–921, 2002.
- [3] R. Livaoglu, "Investigation of seismic behavior of fluid-rectangular tank-soil/foundation systems in frequency domain," *Soil Dyn. Earthquake Eng.*, vol. 28, no. 2, pp. 132–146, 2008.
- [4] A. A. Seleemah and M. El-Sharkawy, "Seismic response of base isolated liquid storage ground tanks," *Ain Shams Eng. J.*, vol. 2, no. 1, pp. 33–42, 2011.
- [5] W. K. Liu and R. A. Uras, "Transient buckling analysis of liquid-storage tanks, Part I. Theory," *Am. Soc. Mech. Eng. Press. Vessels Piping Division (Publication) PVP*, vol. 157, pp. 35–40, 1989.
- [6] A. I. Said and A. A. AbdulMajeed, "Seismic analysis of liquid storage tanks," *J. Eng.*, vol. 17, no. 3, pp. 610–619, 2011.
- [7] S. S. Uddin, "Seismic analysis of liquid storage tanks," *Int. J. Adv. Trends Comput. Sci. Eng.*, vol. 2, no. 1, pp. 357–362, 2013.
- [8] P. J. Cacciatore, L. M. Gustafsson, and A. Kozak, "Seismic response of floating roof storage tanks contact pressure analysis," in *Proceedings of the ASME Pressure Vessels and Piping Conference*, Bellevue, Washington, USA, July 18–22, 2010, pp. 127–138.
- [9] A. A. El-Zeiny, "Factors affecting the nonlinear seismic response of unanchored tanks," in *Proceedings of the 16th ASCE Engineering Mechanics Conference*, University of Washington, Seattle, July 16–18, 2013, pp. 1–9.
- [10] N. Mohammadzadeh, B. J. Amiri, L. E. Endergoli, and S. Karimi, "Coupling tank model and Lars-Weather generator in assessments of the impacts of climate change on water resources," *Slovak J. Civil Eng.*, vol. 27, no. 1, pp. 14–24, 2019.
- [11] S. Kia, M. H. Sebt, and V. Shahhosseini, "Optimization of the infrastructure of reinforced concrete reservoirs by a particle swarm algorithm," *Slovak J. Civil Eng.*, vol. 23, no. 1, pp. 14–22, 2015.
- [12] N. Yukio, *Design Recommendation for Storage Tanks and Their Supports with Emphasis on Seismic Design*. Architectural Institute of Japan, Academia, 2010.
- [13] A. K. Chopra, *Dynamics of Structures: Theory and Applications to Earthquake Engineering*. Harlow: Pearson Education Limited, 2017.
- [14] ABAQUS, User's Manual Version 6.12. Providence: Dassault Systèmes, 2012.
- [15] M. Ismail and H. El-Sokkary, "Seismic retrofit of steel frame structures," *Pollack Period.*, vol. 15, no. 2, pp. 106–117, 2010.
- [16] K. A. Tariq and T. Maki, "Modeling of stress-strain relation of cement-treated sand under compression," *Pollack Period.*, vol. 16, no. 3, pp. 94–100, 2021.
- [17] C. Neagu, F. Dinu, and D. Dubina, D, "Seismic performance of steel plate shear walls structures," *Pollack Period.*, vol. 6, no. 1, pp. 47–58, 2011.
- [18] B. Zhao, "Numerical simulation for the temperature changing rule of the crude oil in a storage tank based on the wavelet finite element method," *J. Therm. Anal. Calorim.*, vol. 107, no. 1, pp. 387–393, 2012.
- [19] B. Bába and T. Karches, "Operation improvement of sequencing FED-batch wastewater treatment," *Pollack Period.*, vol. 16, no. 2, pp. 61–66, 2021.

